

3-1-2018

## Estimating Surface/Subsurface Sediment Mixing in Karst Settings Using <sup>7</sup>Be Isotopes

C. M. Wicks  
*Louisiana State University*

R. L. Paylor  
*Louisiana State University*

S. J. Bentley  
*Louisiana State University*

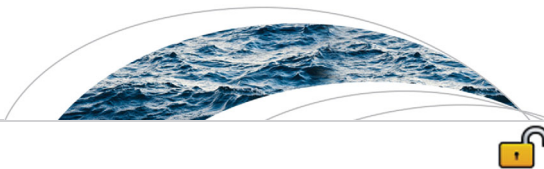
Follow this and additional works at: [https://digitalcommons.lsu.edu/geo\\_pubs](https://digitalcommons.lsu.edu/geo_pubs)

---

### Recommended Citation

Wicks, C., Paylor, R., & Bentley, S. (2018). Estimating Surface/Subsurface Sediment Mixing in Karst Settings Using <sup>7</sup>Be Isotopes. *Water Resources Research*, 54 (3), 2487-2493. <https://doi.org/10.1002/2017WR022192>

This Article is brought to you for free and open access by the Department of Geology and Geophysics at LSU Digital Commons. It has been accepted for inclusion in Faculty Publications by an authorized administrator of LSU Digital Commons. For more information, please contact [ir@lsu.edu](mailto:ir@lsu.edu).



## TECHNICAL REPORTS: METHODS

10.1002/2017WR022192

### Key Points:

- The beryllium-7 sediment tracking method can be used to track suspended sediment in cave streams
- After a 0.78 mm rainfall, up to 52% of the newly deposited sediment along a 3 km-cave stream was surface derived
- During a 4 day runoff event, 22% of the suspended sediment that was discharged had beryllium-7 activities close to those of the soils

### Supporting Information:

- Supporting Information S1

### Correspondence to:

C. M. Wicks,  
cwicks@lsu.edu

### Citation:

Wicks, C. M., Paylor, R. L., & Bentley, S. J. (2018). Estimating surface/subsurface sediment mixing in karst settings using  $^7\text{Be}$  isotopes. *Water Resources Research*, 54, 2487–2493. <https://doi.org/10.1002/2017WR022192>

Received 9 NOV 2017

Accepted 1 MAR 2018

Accepted article online 8 MAR 2018

Published online 23 MAR 2018

© 2018 The Authors.

This is an open access article under the terms of the Creative Commons Attribution-NonCommercial-NoDerivs License, which permits use and distribution in any medium, provided the original work is properly cited, the use is non-commercial and no modifications or adaptations are made.

# Estimating Surface/Subsurface Sediment Mixing in Karst Settings Using $^7\text{Be}$ Isotopes

C. M. Wicks<sup>1</sup> , R. L. Paylor<sup>1</sup>, and S. J. Bentley<sup>1</sup>

<sup>1</sup>Department of Geology and Geophysics, Louisiana State University, Baton Rouge, LA, USA

**Abstract** This study shows that the cosmogenic radionuclide beryllium-7 can be used to track sediment movement through caves. The activities of beryllium-7 and cesium-137 were measured in two different karst settings at both surface and subsurface sites before and after storm runoff events. At one site,  $^7\text{Be}$ -enriched sediment was detected up to 1.5 km along a stream conduit after a moderate storm event; however, the activity of  $^{137}\text{Cs}$  was too variable to show a meaningful pattern. The percentages of surface sediment that was found ranged from 0 to 52% along the entire 3 km cave stream and from 33 to 52% along the upper 1.5 km. At the other site, as much as 96% of the sediment initially discharged at the spring during a storm event was fresh surface material that had traveled into and through the cave stream. Moreover, during the 4 day runoff event, approximately 23% of the total suspended sediment flux was estimated to originate from surface erosion with 78% being reworked sediment from within the cave. The data in this study show that cosmogenic radionuclides with multiyear half-lives are too long-lived to track sediment origins in the caves; whereas,  $^7\text{Be}$  with a 53.2 day half-life, can be used to track movement of sediment along cave streams.

## 1. Introduction

Tracking sediment transport using introduced materials or naturally occurring compounds can be effective tools for analyzing sediment dynamics in karst terrains. A method was developed using lanthanide-tagged sediment to trace clay transport and storage times in karst (Mahler et al., 1998). However, during storm events with high sediment loads, the amount of lanthanide-tagged clay needed for injection can become prohibitive. Other recent methods for tracking fine-grained sediment include application of materials such as microspheres, macrophages, and introduced radioactive compounds (Auckenthaler et al., 2002; Goldscheider et al., 2008; Harvey et al., 2008; Hess, 2008). All of which can be difficult and expensive to implement.

As an alternative to introduced tracers, sediment-tracking using natural tracers can yield significant information on the origin and movement of transported material. Geochemical, biochemical, and physical properties can be used to determine provenance and transformations of sediment (Koiter et al., 2013; Walling, 2013). Selection of an appropriate sediment-tracking technique depends on the questions asked and the temporal and spatial scales addressed. For tracking sediment over short to medium time scales, one of the best options is analysis of short half-life cosmogenic/fallout radionuclides (D'Haen et al., 2012). Sediments stored in karst conduits are cut off from the direct atmospheric fallout of radionuclides (Kaste et al., 2002) potentially allowing exploitation of the contrast between surface and subsurface sediments.

Cosmogenic and fallout radioactive isotopes have been used extensively in surface erosion studies (Guzmán et al., 2013; Mabit et al., 2014) and could be highly effective for determining sediment mixing in karst conduits. The most common isotopes utilized for quantifying moderate to long-term soil erosion and redistribution in the past have been cesium-137 ( $^{137}\text{Cs}$ ,  $T_{1/2} = 30.08$  years; <http://www.nndc.bnl.gov/nudat2/reCenter.jsp?z=55&n=82>) and excess lead-210 ( $^{210}\text{Pb}_{\text{ex}}$ ,  $T_{1/2} = 22.2$  years). These isotopes are a very effective means of tracking sediment movement because these isotopes are adsorbed to soil and sediment particles that are redistributed by physical processes (Mabit et al., 2008). More recently, beryllium-7 ( $^7\text{Be}$ ,  $T_{1/2} = 53.2$  days; <http://www.nndc.bnl.gov/nudat2/reCenter.jsp?z=4&n=3>) has gained attention and research because of its shorter half-life that allows the study of sediment transport at the event scale. Like  $^{137}\text{Cs}$  (Walling & He, 1993) and  $^{210}\text{Pb}_{\text{ex}}$ ,  $^7\text{Be}$  becomes strongly attached to sediment particles and makes an effective chemical

tracer (Walling, 2013; You et al. 1989). In this paper, sediment movement along cave streams was tracked using the cosmogenic radionuclide method.

## 2. Methods

### 2.1. Study Sites

The 6.3 km<sup>2</sup> Sunnybrook Blowing Cave (BC) basin in Wayne County, Kentucky lies at the edge of the Cumberland Escarpment. Land use and land cover in the basin consists of approximately 88% forest, 9% agricultural, and 3% others (Fry et al., 2011). The high gradient, allogenic surface drainage sinks at one swallow hole. All the water from the surface-water basin flows along the cave stream that is in a single conduit. The cave stream is over 3 km long and discharges in the spring (Figure 1). The sediment load consists primarily of silt to cobble size siliciclastic material derived from the surrounding high relief sandstone plateau. Sampling locations included three control sites within the surface-water basin and six in-cave sites along the length of the cave stream. All of the sampling conducted at BC occurred in the fall season of 2011 after a protracted dry period (June–September 2011). There was a small rainfall event on 4 September 2011. Collection of samples of soils (surface reference materials) occurred on 4 and 10 September 2011 (Table 1). Collection of subsurface materials from sites C1 and C6 occurred on 10 September 2011. In mid-November 2011, 37 mm of rain fell over 2 days. Once storm flow subsided, newly deposited sediment was collected by carefully scrapping that sediment into Petri dishes (Broderick, 2016) at six sites along the length of the cave stream. The newly deposited sediment was found on top of sediment banks and was very wet.

The 182 km<sup>2</sup> Hidden River Cave (HRC) basin is located in Hart County, Kentucky. Approximately 85% of the land within the basin is pasture and cropland. Forested lands account for 7%. Communities and developed

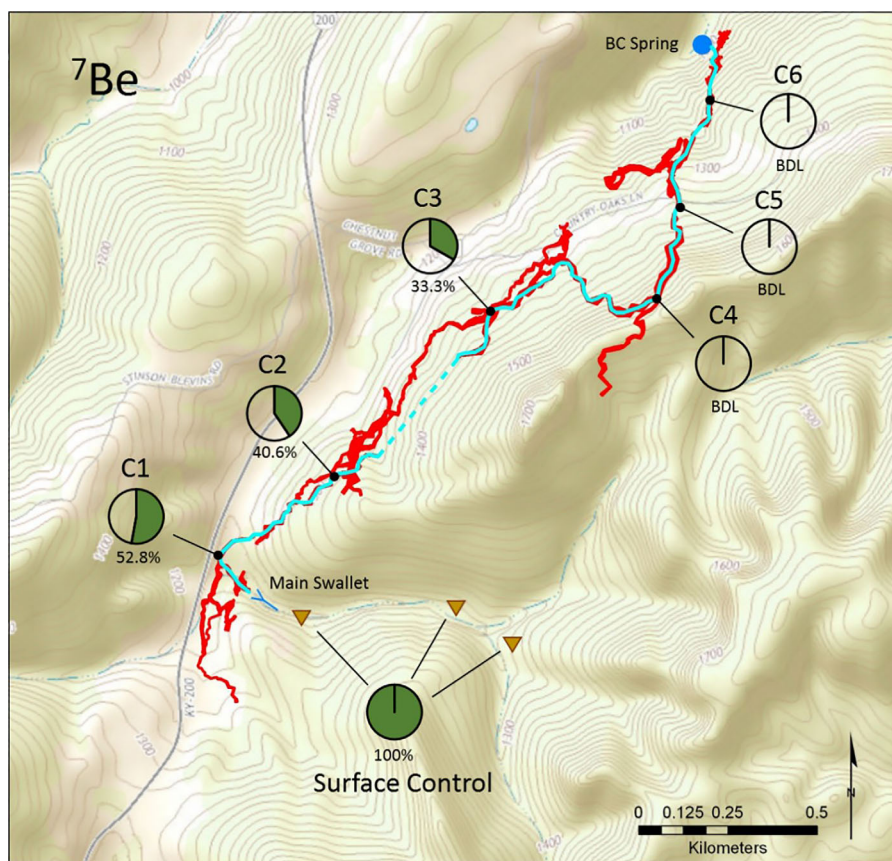


**Figure 1.** Results from the Blowing Cave, Kentucky site showing the percentage of surface-derived material (pie charts) at sampling locations (black dots) along the cave stream (blue line). Access to all locations was along the cave passages (red line). The three surface control samples were collected at the locations shown as inverted gold triangles. Water flows from the main swallet (near C1) toward the spring (large blue dot; near C6).

**Table 1**  
Results From Sampling Event Along a Cave Stream

Sampling time period	Sample location	<sup>7</sup> Be disintegrations per minute per grams (dpm/g)	Percent of control reference	<sup>137</sup> Cs (dpm/g)	Percent of control
Poststorm 4–10 Sep 2011	Surface control	1.783 ± 0.167	100	0.893 ± 0.064	100
Prestorm dry period 4 Sep 2011	C1	ND	ND	ND	ND
	C6	ND	ND	0.159 ± 0.028	17.8
Poststorm 10 Sep 2011	C1	0.539 ± 0.158	30.2	0.129 ± 0.027	14.4
	C6	ND	ND	0.107 ± 0.028	12.0
After moderate storm 20–21 Nov 2011	C1	0.941 ± 0.314	52.8	0.076 ± 0.027	8.5
	C2	0.724 ± 0.201	40.6	0.102 ± 0.020	11.4
	C3	0.594 ± 0.185	33.3	0.266 ± 0.057	29.7
	C4	ND	ND	0.109 ± 0.026	12.2
	C5	ND	ND	0.190 ± 0.035	21.3
	C6	ND	ND	0.074 ± 0.022	8.2

areas account for the remaining 8% (Fry et al., 2011; Raedts & Smart, 2015). The basin lies beneath the town of Horse Cave, KY that has had significant problems with waste disposal including sewage discharge, hexavalent chromium spills from a plating plant (Lewis, 1995), and pesticides, primarily atrazine, from the surrounding agricultural land (Schenk-Brown, 2008). The HRC cave system drains both an extensive sinkhole plain and numerous sinking streams. As is a common occurrence in karst settings, the extent of the mapped cave stream and passages does not extend to edges of the basin nor even to the locations of the sinking streams; therefore, dye tracing is used to prove linkages between surface and subsurface locations. The main cave stream drains an area of ~150 km<sup>2</sup>; the smaller cave stream drains an area of ~8 km<sup>2</sup> (Raedts & Smart, 2015). The straight-line distance between the in-cave sampling location and three surface locations are ~10 km ESE to Blue Spring Creek, ~12 km SSE to Strader Branch, and ~6.5 km SSW to Cave City. Partitioning of storm hydrograph data (gathered with a YSI-6920 logger) allowed estimation of input water sources and event timing. Grab samples for total suspended sediment (TSS) collected at the same time as filtration was completed to generate a calibration curve for the turbidity (NTU) time series from the YSI data.

Following the method of Keller et al. (2017), 5 g of sediment is required for the analyses of <sup>7</sup>Be and <sup>137</sup>Cs attached to sediment. Therefore, field sampling methods were developed that resulted in the collection of a larger mass of sample that when dried would result in more than the required 5 g. The field collection methods also had to account for the fact that some samples were collected from newly deposited material from along the banks of the cave stream; whereas, other samples were collected from the suspended sediment transported in the water column during flood events.

Both background and storm event sampling for suspended sediment were conducted at sinking surface streams and at one location along the main cave stream in HRC. Sampling suspended load (monitoring changes in time at one location) required large volumes of water to obtain sufficient amounts of material for analysis. The minimum target sample size was 5 g or more dried mass, and initial field tests determined the reduction in filter outflow rates that yielded the minimum target mass. For each sample, water was filtered continuously until the flow rate from the filters dropped below 3 L/min (monitored using an in-line Badger flow meter). Leader Ecodiver-750 and 1200 high-volume submersible pumps were operated off field generators or available power supplies with the discharge directed through canister filtration systems. When turbidity was low, standard 5 μm and 1 μm 10 inch polyethylene canister filters were connected in series in order to maximize suspended load capture and reduce sampling times. At higher turbidities, only 5 μm filters were used. Filter sets were sealed and labeled with location, initial dry weight, time, and total pumped volume before transport and laboratory processing.

As the flood pulse receded and the velocity and depth of water decreased, deposition of sediment along the banks of the cave stream can occur. This newly deposited sediment was collected by carefully scraping that sediment into Petri dishes using a small spatula and aiming to scrape no deeper than 1 cm over a 10 cm<sup>2</sup> area (Broderick, 2016). Petri dishes were sealed and labeled with location and time before transport and laboratory processing.

Following the method of Keller et al. (2017), all samples were dried and placed in sealed into plastic petri dishes for analyses on the Canberra BEGe. The specific gamma ray energy emissions from each isotope were analyzed on a Canberra broad energy germanium spectrometer (BEGe 3825 detector, planar geometry) to determine decay counts. Samples were counted for 12–24 h to decrease counting error arising from small sample mass and low radionuclide activities. The resulting number of counts beneath the gamma energy peaks (477.6 keV for  $^7\text{Be}$ , 662 keV for  $^{137}\text{Cs}$ ) were then corrected for instrument detection, sample mass, and decay from time of sampling using standard decay curves. Efficiency calibration for  $^{137}\text{Cs}$  was accomplished via comparison with NIST and IAEA radioisotope standard reference materials. Standard reference materials  $^7\text{Be}$  are not widely available, so efficiency for the 477.6 keV peak was accomplished via interpolation between adjacent peaks for known radioisotopes (Keller et al., 2017).

### 3. Results

One sampling campaign was based on observations of changes in the activity of  $^7\text{Be}$  and  $^{137}\text{Cs}$  of newly deposited fine-grained sediment along a cave stream after a flood event. The other sampling campaign documents temporal changes in the activity of  $^7\text{Be}$  in suspended sediment that is being transported during a flood pulse.

#### 3.1. Blowing Cave: Spatial Variation

The samples collected on 4 September from banks of the cave stream revealed no detectable levels of  $^7\text{Be}$ . These samples were found in the subsurface after a protracted dry period (June 2011 to September 2011) allowing sufficient time for the  $^7\text{Be}$  that was attached to the sediment to decay to levels below detection limits. During the mid-November storm event, there was an influx of sediment that was enriched in  $^7\text{Be}$ . Along 1.5 km of the  $\sim 3$  km flow path,  $^7\text{Be}$ -enriched sediment decreased from 53 to 33% of the surface activity; at the remaining downstream locations, the sediment did not have measurable  $^7\text{Be}$  activity (Figure 1).

Because of the 30.2 year half-life, the prestorm sampling indicated there was still  $^{137}\text{Cs}$  activity in some cave sediments even after the June–September dry period. The levels of  $^{137}\text{Cs}$  found in cave sediments after storm flow were variable and no pattern of mixing or deposition was apparent (Table 1). The random nature of these results is likely due to reworked cave sediment deposited along the banks of the cave stream over a number of years.

#### 3.2. Hidden River Cave: Temporal Variation

In the spring of 2014 and following a 2 week dry period (event 1 in Table 2), suspended sediment was obtained at the in-cave sampling location and at the surface channel of Blue Spring Creek (BSC) in early April 2014 (event 2 in Table 2). Due to the low suspended sediment concentration at both sites, the collection of a sufficient quantity of sediment took more than 3 h at HRC and 2 h at BSC. A moderate rain event occurred during the day on 15 April 2014 with approximately 18 mm of precipitation falling within the drainage basin of HRC. On the morning of 15 April, a suspended sediment sample was obtained at HRC before storm pulse reached the in-cave sampling location with the pump running for 4.7 h to obtain sufficient material due to the very low turbidity (event 3a). In the afternoon of 15 April, surface sampling was conducted at Strader Branch. The sampling was conducted for 1 h as the storm flow was peaking and the turbidity of the water was high (event 3b). An intense spring storm brought 97 mm of precipitation over 13 h and flooding resulted in the HRC basin (28–30 April 2014; Figure 2). Suspended sediment sampling began at the in-cave sampling location at 6 P.M. on 28 April as discharge and turbidity began rising (event 4 in Table 2). The flood in the cave forced abandonment of the sampling effort near midnight on 28 April as the water rose nearly 10 m and inundated the electrical supply box. The sampling effort was resumed the next day using electrical supply from the cave's visitor center. Collection of filtered samples continued for an additional 2 days as the turbid floodwater receded back to normal levels.

Samples collected from the HRC stream conduit during a dry period showed the activity of both  $^{137}\text{Cs}$  and  $^7\text{Be}$  in HRC suspended sediment was low but detectable (0.12 and 1.8 dpm/g, respectively). The activity of  $^{137}\text{Cs}$  and  $^7\text{Be}$  at the BSC surface channel was significantly higher despite lack of recent runoff (0.34 and 11.8 dpm/g, respectively). The  $^{137}\text{Cs}$  and  $^7\text{Be}$  isotope activities were the highest measured at the surface (0.4 and 18.5 dpm/g, respectively), and this data served as the reference control value for estimating ratios of surface/subsurface mixing during the later storm event. During the initial increase in storm-related TSS and

**Table 2**  
Results From Sampling Event During a Storm Event

Month/day/time at start of sampling	Event	<sup>7</sup> Be activity (dpm/g)	<sup>137</sup> Cs activity (dpm/g)	<sup>7</sup> Be in sample relative to the reference (%)	<sup>137</sup> Cs in sample relative to the reference (%)
1–13 April	1	1.8	0.12		
14 April 10:20 <sup>a</sup>	2	11.82 ± 0.59	0.342 ± 0.044	64.0	84.9
14 April 14:41 <sup>b</sup>	2	1.83 ± 0.26	0.119 ± 0.031	9.9	29.5
15 April 9:50 <sup>b</sup>	3a	1.73 ± 0.28	0.139 ± 0.034	9.4	34.5
15 April 15:45 <sup>c</sup>	3b	18.48 ± 0.89	0.403 ± 0.053	100.0	100.0
28 April 18:00 <sup>b</sup>	4	5.45 ± 0.55	0.099 ± 0.019	29.5	24.6
28 April 18:43 <sup>b</sup>	4	11.58 ± 1.07	0.121 ± 0.023	62.7	30.0
28 April 19:40 <sup>b</sup>	4	9.63 ± 0.95	0.251 ± 0.050	52.1	62.3
28 April 20:06 <sup>b</sup>	4	17.80 ± 1.58	0.163 ± 0.032	96.3	40.4
28 April 21:00 <sup>b</sup>	4	11.45 ± 1.04	0.210 ± 0.041	62.0	52.1
28 April 22:07 <sup>b</sup>	4	7.37 ± 0.73	0.237 ± 0.047	39.9	58.8
28 April 22:30 <sup>b</sup>	4	6.86 ± 0.60	0.187 ± 0.038	37.1	46.4
28 April 23:04 <sup>b</sup>	4	10.75 ± 0.73	0.170 ± 0.036	58.2	42.2
29 April 14:35 <sup>b</sup>	4	3.04 ± 0.41	0.212 ± 0.037	16.4	52.6
29 April 15:20 <sup>b</sup>	4	3.07 ± 0.54	0.351 ± 0.045	16.6	87.1
30 April 15:40 <sup>b</sup>	4	2.58 ± 0.45	0.243 ± 0.048	13.9	60.3
1 May 9:10 <sup>b</sup>	4	1.71 ± 0.37	0.193 ± 0.034	9.3	47.9

<sup>a</sup>Blue Spring Creek (swallow hole location). <sup>b</sup>Hidden River Cave stream conduit. <sup>c</sup>Strader Branch (swallow hole location).

the initial decrease in conductance, which indicated that the contribution to runoff from the surface water stream was increasing, the <sup>7</sup>Be activity reached its maximum value. Activities of <sup>7</sup>Be ranged from about 1.7 to 17.8 dpm/g, with an initial spike in material enriched in <sup>7</sup>Be (Figure 2), then reduction of activity at peak turbidity and beyond. The estimated percentages of the storm event suspended sediment derived from surface sources ranged from 9.3 to over 96%. Compared to beryllium-7 results, cesium-137 activity showed

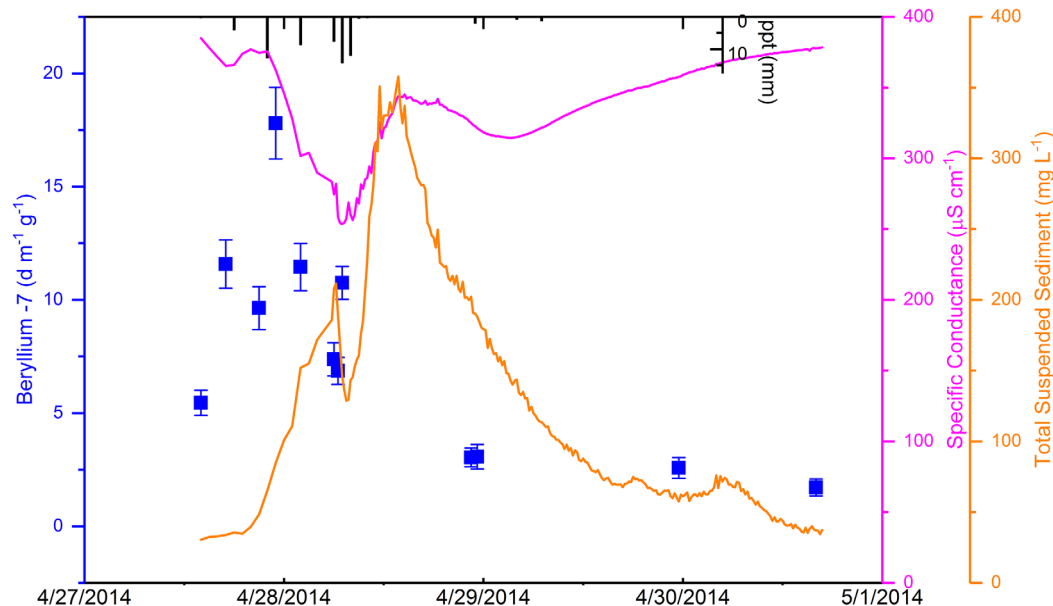


**Figure 2.** Results from Hidden River Cave, Kentucky showing the <sup>7</sup>Be concentration (green squares with error bars), precipitation (black bars), specific conductance (magenta line), and total suspended sediment (orange line). All samples were collected from the stream flowing through the Hidden River Cave stream conduit at the in-cave sampling location. The temporal variation in the mass of total suspended solids (TSS) was calculated from time series turbidity data (measured with data logger) and a calibration curve between the weight of dried suspended sediment and turbidity (supporting information Table S1).

less variability during storm runoff and ranged from about 0.1–0.35 dpm/g. The  $^{137}\text{Cs}$  data were not used to calculate surface/subsurface mixing percentages as the  $^{137}\text{Cs}$  data likely reflect remnant  $^{137}\text{Cs}$  activity in cave sediments from past events as seen in the Blowing Cave system.

#### 4. Conclusions

The minimum particle size of the suspended sediment that was collected and analyzed was either 1  $\mu\text{m}$  (low turbidity conditions) or 5  $\mu\text{m}$  (high turbidity conditions). The relation between particle size and  $^7\text{Be}$  concentrations was not investigated in this study. However, Wittmann et al. (2012) showed that extracted  $^{10}\text{Be}$  concentrations increased 20 times with decreasing particle size (from  $>90\ \mu\text{m}$  to  $<30\ \mu\text{m}$ ). In our study, the lowest  $^7\text{Be}$  concentrations were found under low turbidity conditions, when our method sampled smaller particle sizes. Extrapolating the results of Wittmann et al. (2012) study to  $^7\text{Be}$  and to particle sizes smaller than they sampled, our results might be biased toward yielding higher concentrations. Yet, our results show that these concentrations were the lowest we sampled, so potential bias toward higher concentration due to particle size effect should enhance the difference between the samples collected under lower turbidity conditions (smaller particle size) and higher turbidity conditions (larger particle sizes).

Monitoring beryllium-7 in deposits of sediment along the banks of cave streams and in the suspended sediment flowing past a point in a cave stream is an effective tool for investigating the transport of surface materials into the subsurface and for investigating the mixing of surface and subsurface sediments within karstic basins over short times. An initial field test showed that a moderate storm event moved and deposited fine-grained surface-derived sediment up to upper portion of the Blowing Cave, KY stream conduit. The percentage of surface-derived material ranged from 33 to 53% over the upstream portion (1.5 km) of the cave stream. The farther downstream reaches had no detectable  $^7\text{Be}$  attached to the newly deposited material hinting at remobilization of sediment from within the cave system during the storm event (Fournier et al., 2007). In an investigation of temporal changes, breakthrough of  $^7\text{Be}$ -enriched sediment along the main cave stream preceded the maximum turbidity spike and the dip in specific conductance from rainwater dilution. For the flow event that was studied, surface sediment accounted for an estimated maximum of 96% of total suspended sediment and about 23% of the total sediment flux. Results from using  $^{137}\text{Cs}$  as a sediment tracer were not a clear; however,  $^{137}\text{Cs}$  may be a good tool for estimating flux and transport of surface sediment into karst conduits over longer periods (decades), but more work is needed to account for existing  $^{137}\text{Cs}$ -enriched sediment in the subsurface.

In karst terrains, rapid and turbulent flow into and through well-developed conduits can transport sediment and pollutants in dynamic and unpredictable ways (Kresic, 2013). A better understanding of the rapid changes in sediment flux and transport is needed to provide constraints on related processes such as organic and inorganic carbon transport, soil loss and erosion, sediment-associated pollutant loading, subsurface sediment storage, and ecological impacts. In addition, the mixing of newly eroded surface material with reworked and remobilized sediment stored in subsurface stream conduits and how the provenance of suspended load evolves during storm runoff events are important and poorly studied questions (Herman et al., 2007). Determining the residence times of sediments within conduits and investigating the surface/subsurface sediment mixing ratios in storm runoff has been difficult in karst regions (Herman et al., 2008). Thus, the purpose of this study was to determine the ratios of surface sediment and remobilized subsurface sediment in suspended loads during runoff events.

#### Acknowledgments

Funding was provided by the National Science Foundation grant to CMW. All of the data are provided in the tables. The authors thank the reviewers and our colleagues for their comments on this work.

#### References

- Auckenthaler, A., Raso, G., & Huggenberger, P. (2002). Particle transport in a karst aquifer: Natural and artificial tracer experiments with bacteria, bacteriophages and microspheres. *Water Science and Technology*, 46(3), 131–138.
- Broderick, C. A. (2016). *Tracing sediment in the subsurface using Beryllium-7: Green River basin, KY* (LSU Master's theses). Baton Rouge, LA: Louisiana State University.
- D'Haen, K., Verstraeten, G., & Degryse, P. (2012). Fingerprinting historical fluvial sediment fluxes. *Progress in Physical Geography*, 36(2), 154–186.
- Fournier, M., Massei, N., Bakalowicz, M., Dussart-Baptista, L., Rodet, J., & Dupont, J. (2007). Using turbidity dynamics and geochemical variability as a tool for understanding the behavior and vulnerability of a karst aquifer. *Hydrogeology Journal*, 15(4), 689–704.
- Fry, J. A., Xian, G., Jin, S., Dewitz, J. A., Homer, C. G., Limin, Y., et al. (2011). Completion of the 2006 National land cover database for the conterminous United States. *Photogrammetric Engineering and Remote Sensing*, 77(9), 858–864.
- Goldscheider, N., Meiman, J., Pronk, M., & Smart, C. (2008). Tracer tests in karst hydrogeology and speleology. *International Journal of Speleology*, 37(1), 27–40.

- Guzmán, G., Quinton, J. N., Nearing, M. A., Mabit, L., & Gómez, J. A. (2013). Sediment tracers in water erosion studies: Current approaches and challenges. *Journal of Soils and Sediments*, 13(4), 816–833.
- Harvey, R. W., Metge, D. W., Shapiro, A. M., Renken, R. A., Osborn, C. L., Ryan, J. N., et al. (2008). Pathogen and chemical transport in the karst limestone of the Biscayne aquifer: 3. Use of microspheres to estimate the transport potential of *Cryptosporidium parvum* oocysts. *Water Resources Research*, 44, W08431. <https://doi.org/10.1029/2007WR006060>
- Herman, E. K., Tancredi, J. H., Toran, L., & White, W. B. (2007). Mineralogy of suspended sediment in three karst springs. *Hydrogeology Journal*, 15(2), 255–266.
- Herman, E. K., Toran, L., & White, W. B. (2008). Threshold events in spring discharge: Evidence from sediment and continuous water level measurement. *Journal of Hydrology*, 351(1–2), 98–106.
- Hess, J. W. (2008). Methods in karst hydrogeology. *Groundwater*, 46(2), 172–172.
- Kaste, J. M., Norton, S. A., & Hess, C. T. (2002). Environmental chemistry of beryllium-7. *Reviews in Mineralogy and Geochemistry*, 50(1), 271–289.
- Keller, G., Bentley, S. J., Georgiou, I. Y., Maloney, J., Miner, M. D., & Xu, K. (2017). River-plume sedimentation and  $^{210}\text{Pb}/^{7}\text{Be}$  seabed delivery on the Mississippi River delta front. *Geo-Marine Letters*, 37(3), 259–272.
- Kresic, N. (2012). *Water in Karst: Management, vulnerability, and restoration*. New York, NY: McGraw-Hill.
- Koiter, A., Owens, P., Petticrew, E., & Lobb, D. (2013). The behavioural characteristics of sediment properties and their implications for sediment fingerprinting as an approach for identifying sediment sources in river basins. *Earth-Science Reviews*, 125, 24–42.
- Lewis, J. J. (1995). *The devastation and recovery of caves affected by industrialization* (pp. 217–227). Paper presented at the Proceedings of the 1995 National Cave Management Symposium, Indiana Department of Natural Resources, Spring Mill State Park, IN.
- Mabit, L., Benmansour, M., Abril, J., Walling, D., Meusbürger, K., Iurian, A., et al. (2014). Fallout  $^{210}\text{Pb}$  as a soil and sediment tracer in catchment sediment budget investigations: A review. *Earth-Science Reviews*, 138, 335–351.
- Mabit, L., Benmansour, M., & Walling, D. (2008). Comparative advantages and limitations of the fallout radionuclides  $^{137}\text{Cs}$ ,  $^{210}\text{Pb}$  ex and  $^7\text{Be}$  for assessing soil erosion and sedimentation. *Journal of Environmental Radioactivity*, 99(12), 1799–1807.
- Mahler, B. J., Bennett, P. C., & Zimmerman, M. (1998). Lanthanide-labeled clay: A new method for tracing sediment transport in karst. *Ground Water*, 36(5), 835–843.
- Raedts, C., & Smart, C. (2015). *Tracking of karst contamination using alternative monitoring technologies: Hidden River Cave Kentucky* (pp. 327–336). Paper presented at Proceedings of the 14th Sinkhole Conference, NCKRI Symposium 5, Rochester, MN.
- Schenk-Brown, J. (2008). *Atrazine contamination and suspended sediment transport in Logsdon River: Mammoth Cave, Kentucky* (Masters Thesis & Specialist Projects, Paper 38). Bowling Green, KY: Master of Science, Western Kentucky University.
- Walling, D. (2013). Beryllium-7: The Cinderella of fallout radionuclide sediment tracers? *Hydrological Processes*, 27(6), 830–844.
- Walling, D., & He, Q. (1993). *Use of cesium-137 as a tracer in the study of rates and patterns of floodplain sedimentation* (pp. 319–328). Wallingford, UK: International Association of Hydrological Sciences.
- Wittmann, H., von Blanckenburg, F., Bouchez, J., Dannhaus, N., Christ, M., & Gaillardet, J. (2012). The dependence of meteoric  $^{10}\text{Be}$  concentrations on particle size in Amazon River bed sediment and the extraction of reactive  $^{10}\text{Be}/^9\text{Be}$  ratios. *Chemical Geology*, 318–319, 126–138.
- You, C.-F., Lee, T., & Li, Y.-H. (1989). The partition of Be between soil and water. *Chemical Geology*, 77(2), 105–118.